International Journal of Pharmaceutics 373 (2009) 156–164

Contents lists available at ScienceDirect

International Journal of Pharmaceutics

journal homepage: www.elsevier.com/locate/ijpharm

Pharmaceutical Nanotechnology

Intraoperative therapy with liposomal drug delivery: Retention and distribution in human head and neck squamous cell carcinoma xenograft model

Sean X. Wang[a], Ande Bao[a,b,*], William T. Phillips[b], Beth Goins[b], Stephanie J. Herrera[a,1], Cristina Santoyo[b], Frank R. Miller[a], Randal A. Otto[a]

[a] Department of Otolaryngology–Head and Neck Surgery, University of Texas Health Science Center at San Antonio, 7703 Floyd Curl Drive, San Antonio, TX 78229-3900, USA
[b] Department of Radiology, University of Texas Health Science Center at San Antonio, 7703 Floyd Curl Drive, San Antonio, TX 78229-3900, USA

ARTICLE INFO

Article history:
Received 19 November 2008
Received in revised form 9 February 2009
Accepted 10 February 2009
Available online 21 February 2009

Keywords:
Head and neck squamous cell carcinoma
Intraoperative therapy
Nanoparticle
Liposome
Technetium-99m
Imaging

ABSTRACT

The focus of this study is to investigate the retention and biodistribution of technetium-99m (^{99m}Tc) labeled liposomes in a human head and neck squamous cell carcinoma (HNSCC) positive surgical margin animal xenograft model. Positive surgical margin (with margin < 1 mm) in HNSCC is associated with significant higher mortality and recurrence rate when compared to clear margin. An immediate intraoperative application of liposome-carried therapeutic agents may treat the residual disease intraoperatively and improve long term survival in these patients. To understand the feasibility of this intraoperative therapy in HNSCC, the in vivo behavior of liposomes after intraoperative administration of ^{99m}Tc-labeled liposomes using non-invasive nuclear imaging was investigated in an animal xenograft model. Neutral and cationic ^{99m}Tc-labeled liposomes of 100 nm, 1 μm and 2 μm in diameter (6 study groups with 4 rats per study group) were injected into a nude rat HNSCC positive surgical margin xenograft model. Intratumoral, locoregional, and systemic retention and distribution of the ^{99m}Tc-liposomes were determined using non-invasive nuclear imaging and post-mortem organ distribution. The ^{99m}Tc-liposomes demonstrated high locoregional retention rate of 55.9 ± 3.7% to 72.9 ± 2.4% at 44 h after intraoperative injection to allow significant radiation to the surgical cavity if therapeutic radionuclides were used. Overall, the cationic liposomes demonstrated higher intratumoral retention rate, and the neutral liposomes showed greater retention in the paratumoral cavity ($p < 0.05$ respectively). In conclusion, intraoperative therapy with liposome carried radionuclide drug delivery system carries great potential in treating unresectable HNSCC, and further study using therapeutic radionuclide should be explored.

1. Introduction

Liposomes are a versatile and effective nanometer-scale drug delivery system in modern pharmaceutics (Torchilin, 2007). They minimize drug degradation, increase drug bioavailability, and result in decreased drug toxicity (Torchilin, 2005, 2007). Therapeutic agents encapsulated in liposomes have demonstrated improved pharmacokinetics, greater tumor localization, enhanced therapeutic efficacy, and attenuated side effect profile after intravascular administration (Gabizon et al., 1994; Klibanov et al., 1990; Huang et al., 1992a,b, 1993; Siegal et al., 1995; Vaage et al., 1994). In solid tumors, liposomes are capable of spontaneous intratumoral accumulation via the enhanced permeability and retention (EPR) effect (Maeda, 2001; Maeda et al., 2001). This passive accumulation effect is due to the leaky vasculature of the solid tumors and is further reinforced by the lack of lymphatic system in the tumor, which mainly is responsible for the drainage of macromolecules.

Local administration of liposomal drug delivery has demonstrated a few order increase in sustained retention of liposomes in the tumor (Bao et al., 2006a; Harrington et al., 2000). Liposomes had intratumoral retention of 15.0 ± 12.3% of injection dose in a head and neck squamous cell carcinoma (HNSCC) xenograft model at 96 h following intratumoral injection studied with ^{111}In-labeleing (Harrington et al., 2000). Another study with ^{99m}Tc-labeling has shown a locoregional retention rate of 39.2 ± 10.6% in tumor xenografts at 20 h after intratumoral injection with better intratumoral distribution than unencapsulated ^{99m}Tc-compound (Bao et al., 2006a).

These properties of liposomes may be applicable to the therapy of HNSCC, a solid tumor that carries poor prognosis upon discovery. More than half of the patients with HNSCC are discovered with locally advanced disease, and less than 50% of the patients

* Corresponding author at: Department of Otolaryngology–Head and Neck Surgery, University of Texas Health Science Center at San Antonio, 7703 Floyd Curl Drive, San Antonio, TX 78229-3900, USA. Tel.: +1 210 567 5657; fax: +1 210 567 3617.
E-mail address: bao@uthscsa.edu (A. Bao).
[1] Current address:Department of Otolaryngology–Head and Neck Surgery, University of Texas Health Science Center at Houston, Houston, TX 77030, USA.

0378-5173/$ – see front matter © 2009 Elsevier B.V. All rights reserved.
doi:10.1016/j.ijpharm.2009.02.009

with advanced disease will be cured with combination of surgery, radiation, and/or chemotherapy (Grimard et al., 2006). Complete resection in these patients is often impractical due to the proximity to vital organs such as the carotid artery and the airway leaving them with positive surgical margin that, nevertheless, lead to locoregional recurrence (a major prognostic factor) (Winquist et al., 2007). Traditionally, patients with positive margin receive postoperative radiotherapy and/or chemotherapy; however, the prognosis for these patients remains poor (Jesse and Sugarbaker, 1976). Approximately 75% of patients with positive surgical margin develop local recurrence according to one study (Jones et al., 1996). A retrospective study of 270 patients demonstrated that having a positive margin decreased 5-year disease-free survival from 39% to 7% (Chen et al., 1987). Two major challenges in treating advanced HNSCC are the anatomical limitations of the head and neck and the severe complications associated with large resections and high dose radiation and/or chemotherapy (Freeman et al., 1990; Nag et al., 1998).

To meet the above therapeutic challenges, we focused on intraoperative delivery of therapeutic agents into the tumor or locally around the surgical cavity to treat the areas of the head and neck that are inaccessible or unsafe for complete surgical resection while maintaining tolerable side effect profile. Liposome carried therapeutic agents may be particularly suited for such application.

Recently, a method for directly labeling pH or glutathione (GSH) gradient liposomes with technetium-99m (^{99m}Tc) radioactivity using ^{99m}Tc-*N*,*N*-bis(2-mercaptoethyl)-*N*′, *N*′-diethylethylenediamine (BMEDA) compound without the necessity of further liposome modification was reported (Bao et al., 2003a,b, 2004). ^{99m}Tc is the most commonly used diagnostic radionuclide with 6.02 h physical half life, which emits 141 keV γ-ray for non-invasive nuclear imaging of in vivo distribution at various times. A HNSCC positive surgical margin model in nude rats bearing the HNSCC xenografts was created. In this model, majority of the xenografts were surgically resected followed by intraoperative injection of ^{99m}Tc-liposomes into the remnant tumor and surgical cavity. Non-invasive nuclear imaging and post-mortem organ distribution were used to obtain liposome in vivo distribution and retention at various time points. In this study, we report the biodistribution and retention of two different liposome formulations (neutral and positive surface charges) in three different particle sizes (100 nm, 1 μm and 2 μm in diameter) for a total of 6 nude rat study groups ($n = 4$). We will use the significant findings from this study to discuss the potential application of intraoperative therapy in advanced HNSCC using liposomal therapeutic agents.

2. Materials and methods

2.1. Nude rats and xenograft preparation

The animal experiments reported in the present paper were performed according to the NIH Animal Use Guidelines and were approved by the University of Texas Health Science Center at San Antonio (UTHSCSA) Institutional Animal Care Committee. During all invasive and restrained animal-handling procedures, i.e. tumor cell inoculation, radiotracer injection and animal imaging, the animals were anesthetized with 1–3% of isoflurane (Vedco, St Joseph, MO) in 100% oxygen using an anesthesia inhalation machine (Bickford, Wales Center, NY). The head and neck squamous cell carcinoma cell line, SCC-4, used for HNSCC tumor model is obtained from American Type Culture Collection (ATCC, Manassas, VA). The HNSCC tumor model described in the current research had previously been characterized as a typical squamous cell carcinoma via hematoxylin–eosin (HE) staining and immunohistochemistry of epidermal growth factor receptor (EGFR) (Bao et al., 2006b).

SCC-4 Cells were cultured in Dulbecco's Modified Eagle's Medium (Invitrogen, San Diego, CA) containing 10% fetal bovine serum, 2 mM glutamine, and antibiotics (penicillin and streptomycin) in 100 mm × 20 mm Corning cell culture dishes (Corning Inc., Corning, NY) at 37 °C in a 5% CO_2 atmosphere. When near confluence, cells were trypsinized and collected to determine the number of cells and viability by Trypan Blue dye exclusion assay. The appropriate volume of cell suspension was transferred to a new tube and centrifuged at 800 rpm in an Allegra 21R Centrifuge (Beckman Coulter, Fullerton, CA) at 4 °C for 5 min. Following aspiration of the supernatant, the cell pellets were diluted with saline for injection (Abbott Laboratories, Abbott Park, IL) to a concentration of 5×10^6 cells in 0.2 ml saline. Aliquots of 0.2 ml cell suspension were drawn into tuberculin syringes in preparation for the tumor cell inoculation.

To grow the HNSCC xenografts, each male *rnu/rnu* athymic nude rat (Harlan, Indianapolis, IN) at 4–5 weeks age (75–100 g) was inoculated subcutaneously with 5×10^6 of SCC-4 tumor cells in 0.20 ml of saline on the dorsum at the level of the scapulae. The animals were fed and housed following the protocol for the nude rat living environment at the animal facility at UTHSCSA, and were checked daily after tumor cell inoculation. When the tumor growth in each animal was palpable and of sufficient size to be measured using calipers, the tumor size was obtained by measuring the length (l), width (w) and thickness (t) of each tumor. The tumor volumes were subsequently calculated using the ellipsoid volume formula, $V = (\pi/6)lwt$. When the tumor volume reached approximately 3 cm^3, which typically occurred between 15 and 17 days after tumor cell inoculation, the tumor-bearing animals were then used for study.

2.2. Liposome preparation

Neutrally charged, distearoylphosphatidylcholine (DSPC) liposomes, were comprised of DSPC (Avanti Polar Lipids, Pelham, AL), cholesterol (Calbiochem, San Diego, CA), and Vitamin E (used as an antioxidant) having a molar ratio of 54:44:2. Positively charged 1,2-distearyltrimethyl ammoniumpropane (DSTAP) liposomes were comprised of DSPC, DSTAP (Avanti Polar Lipids, Pelham, AL), cholesterol, and Vitamin E with the molar ratio of 49:5:44:2. Both liposome formulations were prepared as previously described by Bao et al. with modification (2003a). Lipid ingredients were co-dried from chloroform to form a lipid film and desiccated overnight. The dried lipid film was rehydrated with 300 mM sucrose in sterile water at a lipid concentration of 60 mM, warmed to 55 °C and lyophilized overnight. The dried lipid-sucrose mixture was rehydrated with 200 mM glutathione (Sigma, St. Louis, MO) and 300 mM ammonium sulfate (Sigma, St. Louis, MO) in sterile water at 60 mM, subjected to 5 freeze–thaw cycles, and then extruded through a series of polycarbonate filters (2 μm, 2 passes; 1 μm, 2 passes; 400 nm, 2 passes; 200 nm, 2 passes; 100 nm, 5 passes) at 55 °C (Lipex Extruder, Northern Lipids, Canada). The addition of ammonium and GSH was to set up two mechanisms of stably incorporating ^{99m}Tc into liposomes, where ammonium sulfate acted as a pH gradient buffer to increase hydrophilicity of ^{99m}Tc-BMEDA via protonization and GSH could react with ^{99m}Tc-BMEDA resulting in hydrophilic ^{99m}Tc-BMEDA/GSH.

At each desired particle size an aliquot was removed and passed at least 5 times through the filter. The remaining liposomes were extruded through the next filter size. After extrusion, the liposomes at the various sizes were repeatedly washed in 300 mM ammonium sulfate in sterile water and centrifuged at 41,000 rpm for 50 min to remove any unencapsulated glutathione. Liposome pellets were resuspended in 300 mM ammonium sulfate containing 300 mM sucrose in sterile water at a total lipid concentration of 60 mM and stored at 4 °C until needed.

Table 1
The average %IA at 44 h after intraoperative injection (average ± S.D., $n = 4$ for each).

Liposome Formulation	Diameter (nm)	^{99m}Tc-Labeling Efficiency	Average Tumor Size (cm^3)	Residual Tumor Size (g)	% Injected Activity
100 nm Cationic	130.5 ± 18.1	66.1	1.6 ± 0.5	0.5 ± 0.1	55.9 ± 3.7
100 nm Neutral	109 ± 11.1	66.9	5.1 ± 0.3	0.8 ± 0.6	62.1 ± 2.6
1 μm Cationic	1196 ± 153.6	54.3	6.1 ± 1.2	1.3 ± 0.5	63.0 ± 4.2
1 μm Neutral	868.0 ± 74.9	51.9	3.2 ± 0.3	0.8 ± 0.3	67.1 ± 3.5
2 μm Cationic	2026.7 ± 297.5	51.0	4.8 ± 0.3	1.5 ± 0.2	71.5 ± 5.6
2 μm Neutral	1398.5 ± 104.1	72.6	3.3 ± 1.3	0.7 ± 0.4	72.9 ± 2.4

Following manufacture, liposome size was measured using a 488 nm laser light scattering instrument (Brookhaven Instruments, Holtsville, NY) and are shown in Table 1. Phospholipid content was measured using Stewart assay (Stewart, 1980). Liposomes were also checked for endotoxin levels and bacterial growth. No growth of bacteria was detected in 14-day culture and endotoxin levels were <2.5 EU/ml.

2.3. Preparation of ^{99m}Tc-BMEDA

The method used to prepare the ^{99m}Tc-BMEDA was the same as previously described by Bao et al. with minor modifications (2006a). In brief, the process was as follows: 50 mg of sodium glucoheptonate (GH) (Sigma, St. Louis, MO) and 3.5 μl of BMEDA (synthesized in house) were combined in the same vial, followed by the addition of 5.0 ml of normal saline for injection (nitrogen gas-flushed in advance). Following 20 min of magnetic stir mixing, 60 μl of freshly prepared degassed stannous chloride (Aldrich, Milwaukee, WI) solution (15 mg/ml) was added to the GH–BMEDA solution, followed by pH adjustment using 0.05 M sodium hydroxide to achieve a pH ranging between 7 and 8. At that point, 1.0 ml of the resulting solution was transferred to a glass vial containing 0.60 ml of 2.22 GBq (60 mCi) ^{99m}Tc-pertechnetate (GE Healthcare, San Antonio, TX). The mixed solution was incubated at 25 °C for 20 min with intermittent gentle shaking. The labeling efficiency of the ^{99m}Tc-BMEDA was found to be over 80% employing paper chromatography eluted with methanol or saline. The ^{99m}Tc-BMEDA was then used immediately for liposome labeling.

2.4. Preparation of ^{99m}Tc-liposomes

For a typical labeling study, 1.0 ml of liposomes (60 mM of total lipids) prepared as described above were separated to remove free ammonium sulfate from liposomes by elution with phosphate buffered saline (PBS), pH 7.4 via disposable Sephadex G-25 column chromatography (Amersham Biosciences, Uppsala, Sweden). The product was added to the ^{99m}Tc-BMEDA solution and incubated at 37 °C for 1 h. Again, the ^{99m}Tc-liposomes were separated from any unencapsulated ^{99m}Tc-BMEDA via disposable Sephadex G-25 column chromatography eluted with PBS buffer, pH 7.4. The radiolabeling efficiencies are shown in Table 1.

2.5. Positive surgical margin model and ^{99m}Tc-liposomes injection

At approximately 2 weeks after SCC-4 cells injection, the nude rats were prepared for partial surgical resection of the xenograft. The average tumor size at 2 weeks for the 100 nm, 1 μm, and 2 μm neutral liposome rats were 5.1 ± 0.3 cm^3, 3.2 ± 0.3 cm^3, and 3.3 ± 1.3 cm^3 respectively. The average tumor size for 100 nm, 1 μm, and 2 μm cationic liposome rats were 1.6 ± 0.5 cm^3, 6.1 ± 1.2 cm^3, and 4.8 ± 0.3 cm^3 respectively. All instruments were autoclaved, and the operating area was maintained in a sterile environment. A transverse incision directly superior to the tumor was used to open the skin. To create the positive margin model, 0.5–1.0 g of residual tumor was maintained and injected with ^{99m}Tc-liposomes. The residual tumor sizes for the 100 nm, 1 μm, and 2 μm ^{99m}Tc-neutral liposome groups were 0.8 ± 0.6 g, 0.8 ± 0.3 g, and 0.7 ± 0.4 g respectively, and for the 100 nm, 1 μm, and 2 μm ^{99m}Tc-cationic liposome group, the remaining tumor weight were 0.5 ± 0.1 g, 1.3 ± 0.5 g, and 1.5 ± 0.2 g respectively. After tumor resection, 0.5 ml of ^{99m}Tc-liposomes with average activity of 577.2 ± 59.2 MBq/kg (15.6 ± 1.6 mCi/kg) body weight were injected using 1-ml tuberculin syringe with skin retracted. The skin was closed immediately using interrupted sutures (3-O silk).

2.6. Retention and distribution of the ^{99m}Tc-liposomes

Planar gamma camera images, SPECT images, and CT images were acquired using a dual head microSPECT/CT scanner (XSPECT, Gamma Medica, Northridge, CA). Static images in lateral view were acquired at baseline (2 min acquisition), 4 h (2 min acquisition), 20 h (10 min acquisition), and 44 h (30 min acquisition) using a low energy high resolution parallel hole collimator. During each static image acquisition, a standard (average activity of 11.1 ± 0.0 MBq (0.3 ± 0.0 mCi)) ^{99m}Tc-source was positioned outside the animal but still within the field of view for image quantification.

At 4-h following the intraoperative injection into the residual tumor and, immediately following static image acquisition, 1-mm pinhole collimator SPECT images were acquired, with the center of the field of view (FOV) focused on the tumor of each animal. The radius of rotation (ROR) was maintained around 5.30 cm with a FOV approximately 5.00 cm. This was accomplished using 60 s per projection for a total of 64 projections around the rat (dual head 32 projections each; 180° rotation).

The SPECT imaging was followed by CT image acquisition (X-ray source: 80 kVp, 280 mA; 256 projections) while precisely maintaining the positioning of the animal. The software provided with microSPECT/CT was used for the SPECT and CT image reconstruction including the SPECT/CT image fusion. The SPECT images were reconstructed to produce image sizes of 56 × 56 × 56 with an image resolution of 0.95 mm. The CT images were also reconstructed, resulting in image sizes of 512 × 512 × 512 with a 0.15 mm image resolution. The percentage of ^{99m}Tc activity retained in the tumor and the surrounding tissues across time was calculated from static images created by drawing the region of interest (ROI) using the standard source as a point of reference.

Forty-four hours following intraoperative injection, each animal was euthanized by cervical dislocation under deep isoflurane anesthesia. The major organs including the liver, spleen, kidneys, heart and lungs were collected. The tumor itself, the fluid within the surgical cavity, the skin immediately superior to the tumor, and the musculature inferior to the tumor were also collected. Activity at each of these sites was measured with a Wallac 1480 Wizard 3″ automatic well gamma counter (Perkin-Elmer Life Sciences, Boston, MA). The percent of injected activity per gram of tissue and percent of injected activity per organ was calculated as described by Bao et al. (2003b).

2.7. Intracavitary ^{99m}Tc-liposome injection groups

In order to study the effect of the electrostatic charge on the ^{99m}Tc-liposome in vivo distribution without being skewed by injec-

tion technique, two additional groups of rats, 100 nm ^{99m}Tc-neutral liposome and 100 nm ^{99m}Tc-cationic liposome, were studied by injecting the ^{99m}Tc-liposomes directly into the surgical cavity. To ensure that the study methods were comparable, all procedures, both ante- and post-mortem, were duplicates of those carried out with the six groups that were intratumorally injected except for the following differences: (1) the two intracavitary injected rats were sacrificed at 20 h, and (2) an additional planar image at 20 h and SPECT/CT at 20 h were taken for selected rats after the tumor was completely resected from the body. After tumor was resected, the rat was placed back on the microSPECT/CT scanner with a foam inserted between the resected tumor and the muscle to allow complete visualization of the activity distribution within the tumor.

2.8. Statistical analysis

The data are presented as the mean value ± one standard deviation (S.D.). Origin statistical software (Version 7.5) (Origin Lab, Northampton, MA) was used for the calculation of the means, standard deviations, and statistical analysis. The data with regard to different experiment groups were tested with 2-sample Student-*t* test. Statistical significance uses a 95% confidence interval ($p < 0.05$).

3. Results

3.1. Locoregional retention by planar imaging

The locoregional (tumor, skin superior to the tumor, fluid within the surgical cavity, and muscle inferior to the tumor) percent injected activity (%IA) at baseline, 4 h, 20 h and 44 h were derived from planar images by drawing ROI. The planar images were acquired laterally, and the locoregional, kidney, liver, and standard can be clearly differentiated. Fig. 1 shows the average locoregional %IA for the 6 different nude rat groups from baseline to 44 h. The activity cleared from the initial injection site in 2 stages. All groups displayed the greatest decrease in activity within the first 4 h (10.0 ± 4.2%). Between 4 h and 44 h, an average of 21.0 ± 4.2%IA was lost. The rate of activity dissipation was not significant between different groups. Overall, the locoregional retention of the ^{99m}Tc-liposomes followed a second order exponential decay model ($R^2 = 0.999$) with the following general formula:

$$y = y_0 + A_1 e^{-x/t_1} + A_2 e^{-x/t_2}$$

where y_0 represents the *Y* offset (i.e. the constant retention activity other than the cleared components following the exponential decay mechanism), A_1 and A_2 represent the percentage of activity which were cleared with decay constants of t_1 and t_2 respectively for ^{99m}Tc-liposomes. Subsequently, the half clearance times correlated with the radioactivity components of A_1 and A_2 are $t_1 \times 0.693$ and $t_2 \times 0.693$ correspondingly. At any given point, the locoregional retention for the ^{99m}Tc-neutral liposome groups was consistently higher than the ^{99m}Tc-cationic liposome groups of the same particle size. Table 1 lists the average locoregional %IA for each of the 6 liposome groups at 44 h. The overall mean for all rats at 44 h was 65.1 ± 6.8%, and the retention rate ranged from 55.9 ± 3.7% (100 nm cationic liposomes) to 72.9 ± 2.4% (2 μm neutral liposome). The 100 nm ^{99m}Tc-neutral liposome group had significantly higher locoregional retention compared to the 100 nm ^{99m}Tc-cationic liposome group ($p < 0.05$), and the larger ^{99m}Tc-liposomes had higher retention rate than smaller ^{99m}Tc-liposomes of the same charge.

3.2. Organ retention by gamma counter

After the rats were sacrificed at 44 h, the organs were resected, and their activity was recorded using a gamma counter. The activity measured from the counter was used to calculate (based on the activity in the standard) the %IA per organ (Fig. 2) and the percent injected activity per gram (%IA/g) of tissue for the locoregional tissues (Fig. 3). When the individual organs were analyzed, the tumors of the ^{99m}Tc-cationic liposome groups had higher %IA per organ and %IA/g of tissue than the ^{99m}Tc-neutral liposome groups of the same size (Fig. 2). The average %IA per organ for the tumors ranged from 6.9 ± 2.1%, for the 100 nm ^{99m}Tc-neutral liposome group, to 52.2 ± 15.4%, for 2 μm cationic liposome group. In contrast to the tumor %IA, the 100 nm and 1 μm ^{99m}Tc-neutral liposome groups had higher activity in the intracavitary fluid than the 100 nm and 1 μm ^{99m}Tc-cationic liposome groups respectively. The fluid of the 100 nm and 1 μm ^{99m}Tc-neutral liposome groups had 9.1 ± 6.5% and 8.0 ± 8.7%IA per organ respectively compared to 0.2 ± 0.3% and 0.8 ± 0.5% respectively for the 100 nm and 1 μm ^{99m}Tc-cationic liposome groups. The fluid activity for the 2 μm ^{99m}Tc-neutral liposome group (1.3 ± 0.9%) was not significantly different compared to the 2 μm ^{99m}Tc-cationic liposome group (1.6 ± 0.9%). The difference between the %IA per organ for the various liposome formulations was less well defined for the muscle inferior to the tumor and the skin superior to the tumor.

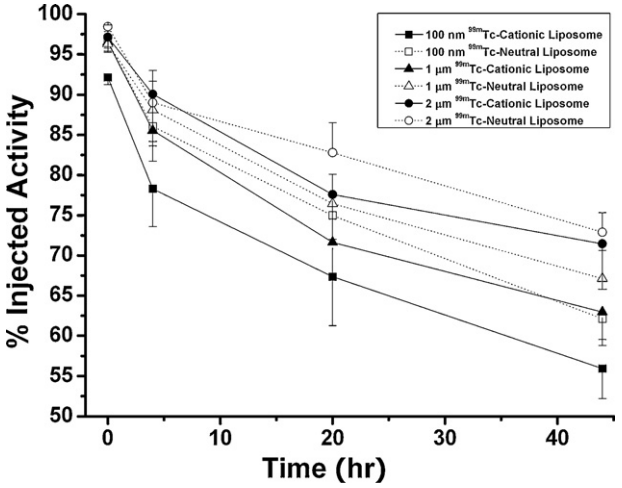

Fig. 1. The locoregional (tumor, fluid, skin, and muscle) percent of administered activity up to 44 h calculated using ROI analysis of planar gamma camera images of tumor-bearing rats in a lateral position. The DSPC liposomes have higher locoregional retention rates compared to their DSTAP counter parts.

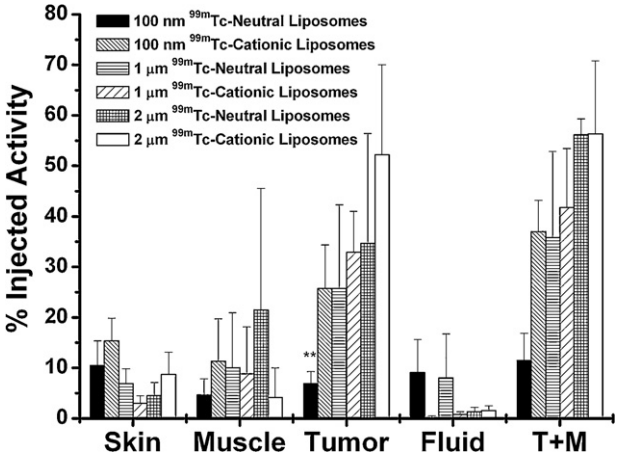

Fig. 2. Average %IA/organ for each group (4 rats within each group) of rats. Skin was taken above the tumor, and muscle was taken below the tumor. Fluids were suctioned during tumor dissection. The tumor activity/organ value was higher for the DSTAP group compared to DSPC group of the same liposome size. The two smallest 100 nm groups had the largest activity/organ discrepancy.

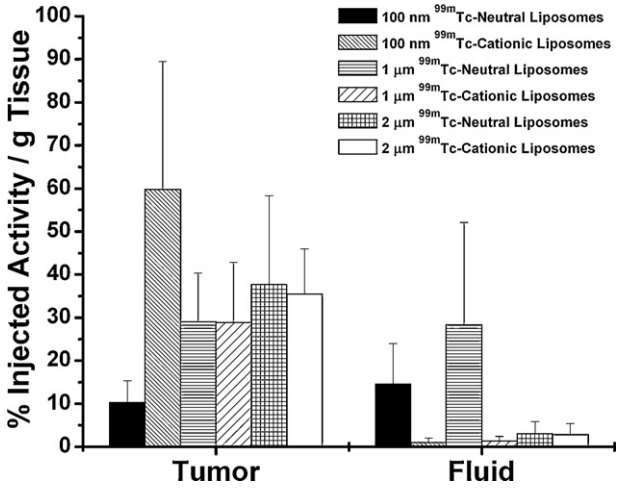

Fig. 3. Average %IA/g tumor and intracavitary fluid for each ^{99m}Tc-liposome rat group ($n = 6$). The 100 nm DSTAP ^{99m}Tc-liposome rats have the highest %/g value indicating high retention rates and potentially greater therapeutic effect. The 100 nm DSPC ^{99m}Tc-liposome rats have higher %/g value compared to the 100 nm DSTAP ^{99m}Tc-liposome rats demonstrates neutrally charged liposomes have greater tendency to leak out of the tumor.

The tumor %IA/g of tissue (Fig. 3) ranged from 10.2 ± 4.4%, for the 100 nm neutral liposome, to 59.8 ± 25.7%, for the 100 nm cationic liposomes (the mean postoperative tumor size was not significantly different for the 2 groups ($p > 0.05$)). The 100 nm ^{99m}Tc-cationic liposome group had significantly higher tumor ($p < 0.05$) %IA/g of tissue compared to the 100 nm ^{99m}Tc-neutral liposome group. The cationic and neutral 1 μm and 2 μm ^{99m}Tc-liposome groups had insignificant difference in their average %IA/g of tissue value when compared to each other (Fig. 3). When the %IA/g of tissue was calculated for the intracavitary fluid, a similar relationship to the percent per organ value was found. The 100 nm (14.6 ± 9.4%) and 1 μm (28.3 ± 23.8%) ^{99m}Tc-neutral liposome groups had significantly higher ($p < 0.05$) value than the 100 nm (1.0 ± 1.0%) and 1 μm (1.3 ± 1.1%) ^{99m}Tc-cationic liposome groups respectively. The 2 μm ^{99m}Tc-neutral liposome group and the 2 μm ^{99m}Tc-cationic liposome group were not significantly different at 2.9 ± 2.8% and 2.8 ± 2.6% respectively.

Based on the percent per organ and percent per gram of tissue data, the ^{99m}Tc-cationic liposomes appear to have better intratumoral retention, and the ^{99m}Tc-neutral liposomes seem to leak out of the tumor into the surrounding surgical cavity more readily. However, we were not sure if our injection technique could have contributed to this difference. To verify this assumption, two additional experimental groups (100 nm ^{99m}Tc-cationic and 100 nm ^{99m}Tc-neutral liposomes) were created to directly inject the ^{99m}Tc-liposomes into the surgical cavity after tumor was resected instead of intratumoral injection, removing the human errors during injection that could alter the distribution pattern.

3.3. Organ retention in two groups receiving intracavitary injection

The %IA per organ (Fig. 4A) and %IA/g of tissue (Fig. 4B) were derived from the gamma counter for the 100 nm ^{99m}Tc-cationic liposome group and the 100 nm ^{99m}Tc-neutral liposome group via injection into the surgical cavity. The average tumor %IA per organ for the ^{99m}Tc-cationic liposome group and ^{99m}Tc-neutral liposome group were 18.6 ± 4.3% and 2.9 ± 2.5% respectively at 20 h with the cationic group having a significantly higher ($p < 0.05$) retention rate, and the tumor %IA/g of tissue were 16.2 ± 3.5% and 2.0 ± 1.1% respectively. Fig. 5 shows the MicroSPECT/CT fusion images comparing the

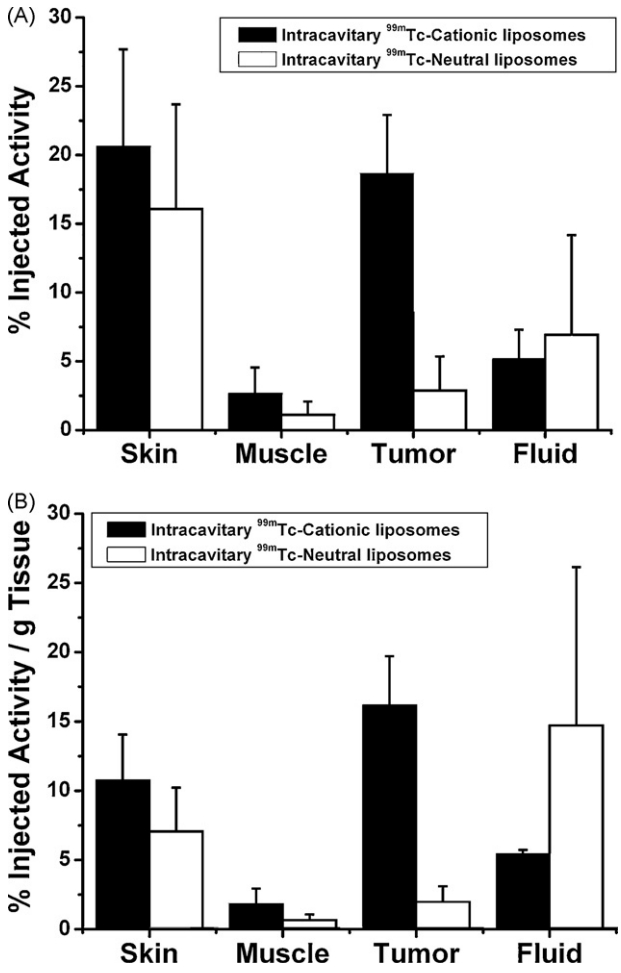

Fig. 4. When radionuclide liposomes were injected directly into the cavity, the rats injected with DSTAP ^{99m}Tc-liposomes had both higher %IA/organ (A) and %IA/g of tissue (B) in the tumor compared to DSPC ^{99m}Tc-liposome. However, the DSPC ^{99m}Tc-liposome had higher %IA/organ and %IA/g of tissue than DSTAP ^{99m}Tc-liposome. These results indicated that the positive charged DSTAP ^{99m}Tc-liposomes had a greater affinity toward tumor tissue than the neutrally charged DSPC ^{99m}Tc-liposome.

activity distribution of the 100 nm ^{99m}Tc-neutral liposome group and the 100 nm ^{99m}Tc-cationic liposome group at 20 h. The tumor was resected from the rat and placed on top of a foam to separate the tumor from the tissue beneath. The fusion image clearly demonstrates a greater amount of activity within the tumor of the ^{99m}Tc-cationic liposome rat versus the ^{99m}Tc-neutral liposome rat.

The average fluid %IA per organ for the 100 nm ^{99m}Tc-neutral liposome and 100 nm ^{99m}Tc-cationic liposome group were 6.9 ± 7.2% and 5.1 ± 2.2% respectively, and the %IA/g of tissue values were 14.7 ± 11.4% and 5.4 ± 0.3% respectively. In contrary to the tumor retention rate, the neutral group had higher fluid injected activity.

3.4. Systemic organ distribution by planar imaging

The systemic distribution of %IA in the kidney and the liver at major time points (baseline, 4 h, 20 h, and 44 h) were determined in the same fashion as the tumor using planar imaging. The average %IA in the kidney (Fig. 6A) at baseline, 4 h, 20 h and 44 h for all six groups were 0.9 ± 0.6%, 1.8 ± 0.8%, 2.2 ± 0.7%, and 2.2 ± 0.8% respectively. The highest value at any time point was 3.3 ± 1.3% at 44 h for the 100 nm ^{99m}Tc-cationic liposome group. Fig. 6A shows

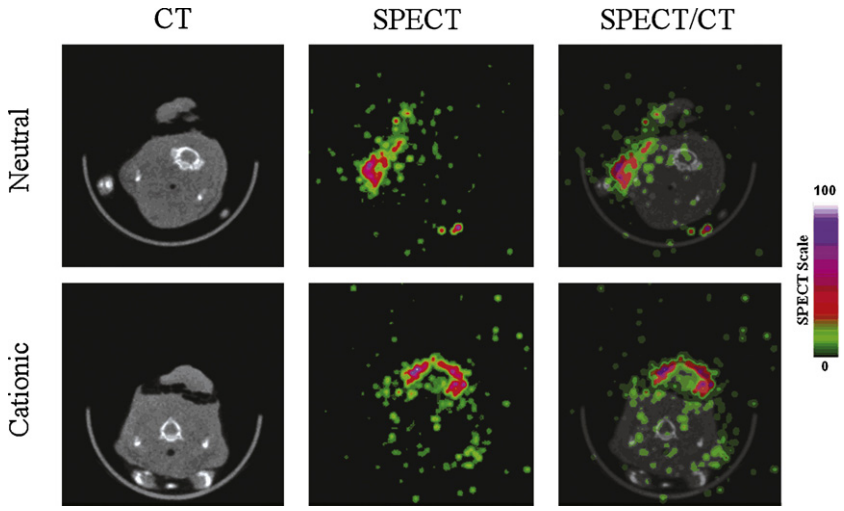

Fig. 5. Micro-CT, pinhole collimator SPECT, and fusion images (axial) of tumor-bearing rats acquired at 20 h post-intracavitary injection of the 100 nm ^{99m}Tc-neutral liposomes (upper panel) and 100 nm ^{99m}Tc-cationic liposome (lower panel). The images were taken immediately after rats were sacrificed with a foam placed inferior to the resected tumor to delineate the tumor from rest of the animal. The pinhole collimator SPECT images were focused on the tumor in each animal. The color scale shows the SPECT and CT values from 0% to maximum expressed with an arbitrary 100%. The SPECT pixel values beyond the color range of the map are shown in white. The ^{99m}Tc-cationic liposome group demonstrated higher intratumoral activity compared to the ^{99m}Tc-neutral liposomes group even though the activity was injected into the surgical cavity instead of the tumor.

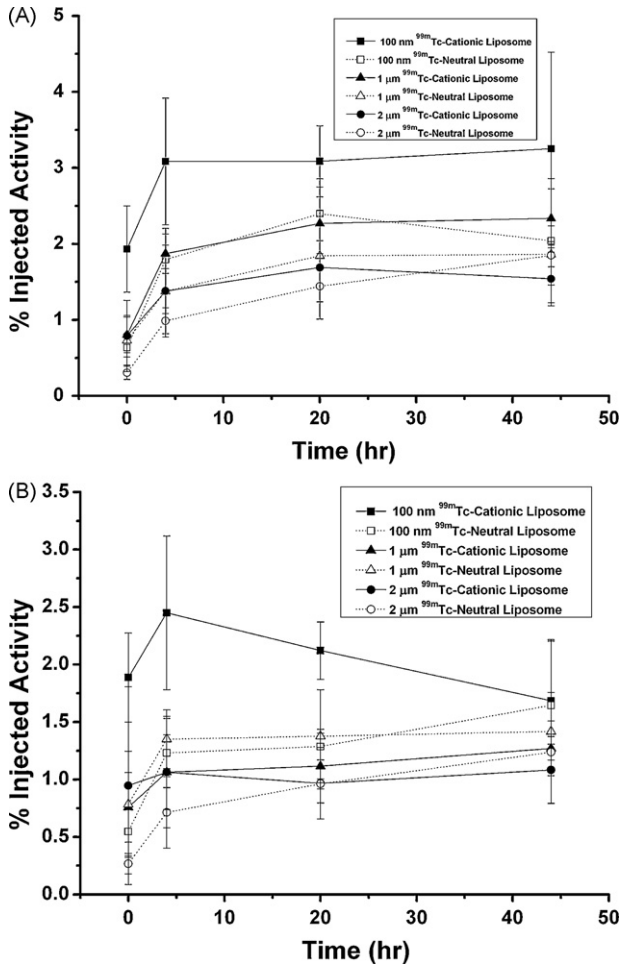

Fig. 6. The kidney %IA per organ (A) and liver %IA per organ (B) based on lateral planar gamma imaging are plotted from baseline to 44 h post injection. At any given point, the average amount of activity in kidneys does not exceed 5% total activity. The liver had even less activity. This shows that liposomal radionuclides have minimal systemic distribution.

that the %IA increased quickly from baseline to 4 h, and then the activity leveled off from 4 h to 44 h.

The average %IA in the liver (Fig. 6B) at baseline, 4 h, 20 h and 44 h for all six groups were $0.9 \pm 0.7\%$, $1.3 \pm 0.7\%$, $1.3 \pm 0.5\%$, and $1.4 \pm 0.4\%$ respectively. The highest value at any time point was $1.7 \pm 0.5\%$ at 44 h for the 100 nm ^{99m}Tc-cationic liposome group. The liver, similar to the kidney, demonstrated an initial rise in %IA within the first 4 h, and then most groups stabilized.

3.5. Systemic distribution by gamma counter

Activity for all systemic organs was acquired by a gamma counter at 44 h after the animals were euthanized, and the %IA per organ (Table 2) and the %IA/g of tissue were derived from the activity count. The kidney values were similar to the %IA derived from planar imaging with an overall average of $2.1 \pm 1.0\%$. The 100 nm ^{99m}Tc-cationic liposome group was the highest at $3.8 \pm 0.5\%$, and the 2 μm ^{99m}Tc-cationic liposome group was the lowest at $1.1 \pm 0.0\%$. The liver showed overall average of $1.5 \pm 0.4\%$ injected activity per organ similar to the value from planar image. The 100 nm ^{99m}Tc-cationic liposome group had the highest %IA per organ value for liver at $2.0 \pm 0.1\%$, and the 2 μm ^{99m}Tc-cationic liposome group was the lowest at $1.2 \pm 0.5\%$. The percent per organ activity for the whole gastrointestinal tract was calculated by summing the values for intestine, stomach, and cecum. The average gastrointestinal tract %IA per organ for all rats was $1.2 \pm 0.5\%$. Again the 100 nm ^{99m}Tc-cationic liposome group had the highest %IA with $2.1 \pm 0.1\%$, and the 2 μm ^{99m}Tc-cationic liposome group had the lowest value of $0.8 \pm 0.1\%$. The activities in other organs were significantly lower compared to kidney, liver, and gastrointestinal tract (Table 3).

4. Discussion

The interior of liposome has the versatility to house a variety of therapeutic agents, including chemotherapeutic agents and therapeutic radionuclides (Torchilin, 2005). The ^{99m}Tc-BMEDA radiolabeling method for liposomes (Bao et al., 2003a, 2004), based on pH or GSH gradient, can reliably track in vivo liposome activity. Since pH gradient is a commonly used method to load therapeutic agents into liposomes with high capacity and high efficiency, this radiolabeling method has a significant advantage for the direct

Table 2
Major normal organ distribution at 44 h after intraoperative injection (average ± S.D., $n = 4$ for each). When the %IA per organ was measured using the gamma counter at 44 h, overall activity was low in all the major systemic organs. Kidney had the highest activity. The low systemic organ retention predicts minimal normal organ toxicity for intraoperative injection of liposomal radionuclide.

Organs	100 nm Cationic (%IA)	100 nm Neutral (%IA)	1 μm Cationic (%IA)	1 μm Neutral (%IA)	2 μm Cationic (%IA)	2 μm Neutral (%IA)
Intestine	0.7 ± 0.1	0.5 ± 0.1	0.3 ± 0.1	0.3 ± 0.1	0.2 ± 0.1	0.5 ± 0.2
Stomach	0.1 ± 0.0	0.1 ± 0.0	0.1 ± 0.0	0.1 ± 0.0	0.0 ± 0.0	0.0 ± 0.0
Cecum	1.4 ± 0.1	0.8 ± 0.2	0.6 ± 0.1	0.6 ± 0.3	0.6 ± 0.1	0.6 ± 0.1
Kidney	3.8 ± 0.5	2.4 ± 0.3	2.1 ± 0.3	1.6 ± 0.1	1.1 ± 0.0	1.4 ± 0.1
Spleen	0.1 ± 0.0	0.1 ± 0.0	0.0 ± 0.0	0.1 ± 0.0	0.1 ± 0.1	0.0 ± 0.0
Liver	2.0 ± 0.1	1.7 ± 0.4	1.2 ± 0.2	1.6 ± 0.5	1.2 ± 0.5	1.3 ± 0.1

Table 3
Major normal organ %IA/g of tissue at 44 h after intraoperative injection (average ± S.D., $n = 4$ for each). Percent per gram of tissue may be a better predicator of systemic organ side effect in clinical setting since it is not skewed by the size of the organ. The %IA/g for all the systemic organs is less than 0.5 except for kidney. In humans, the kidney size is 100 times the size of a rat's kidney thus less activity is expected.

Organs	100 nm Cationic (%IA/g)	100 nm Neutral (%IA/g)	1 μm Cationic (%IA/g)	1 μm Neutral (%IA)	2 μm Cationic (%IA)	2 μm Neutral (%IA)
Intestines	0.1 ± 0.0	0.1 ± 0.0	0.0 ± 0.0	0.0 ± 0.0	0.0 ± 0.0	0.0 ± 0.0
Stomach	0.0 ± 0.0	0.0 ± 0.0	0.0 ± 0.0	0.0 ± 0.0	0.0 ± 0.0	0.0 ± 0.0
Cecum	0.2 ± 0.0	0.1 ± 0.0	0.1 ± 0.0	0.1 ± 0.0	0.1 ± 0.0	0.1 ± 0.0
Kidney	1.9 ± 0.3	1.3 ± 0.2	0.9 ± 0.2	0.8 ± 0.1	0.5 ± 0.1	0.7 ± 0.0
Spleen	0.1 ± 0.0	0.1 ± 0.1	0.1 ± 0.0	0.1 ± 0.0	0.1 ± 0.1	0.1 ± 0.0
Liver	0.2 ± 0.0	0.2 ± 0.0	0.1 ± 0.0	0.2 ± 0.0	0.1 ± 0.0	0.1 ± 0.0

labeling of drug carrying liposomes without the necessity of additional modification to the drug delivery liposomes (Bao et al., 2004), which avoids the influence of in vivo behavior by liposome formulation/surface modification. In addition, this method can also be used to encapsulate therapeutic radionuclides, ^{186}Re and ^{188}Re, into liposomes for cancer radionuclide therapy with liposome drug delivery (Bao et al., 2003b; Wang et al., 2008).

In advanced HNSCC, positive surgical margin is associated with markedly higher mortality compared to those with negative margins (54% versus 29%) (Haque et al., 2006). One of the major problems with positive margin is that it inevitably predicates cancer recurrence, a major prognostic factor in HNSCC (Jones et al., 1996). Studies have shown that gross margin has significantly higher local recurrence rate compared to clear or microscopic margins (Nag et al., 2005). In such cases, salvage therapy with radiation therapy and/or systemic chemotherapy is often associated with unacceptable complications and is further limited in the head and neck anatomy. Therefore, intratumoral injection has an obvious appeal in the treatment of HNSCC by achieving high drug concentration at the site of action thus improving therapeutic efficacy and reducing normal tissue toxicity.

However, the direct intratumoral injection of a therapeutic agent has yet to establish a role in the standard treatment of HNSCC. This paradox can be explained by the inability to achieve adequate locoregional retention of the agent at the site and the concern for normal-tissue toxicity both locally and systemically. Various attempts, including the use of vasoconstrictors, have been made to improve local retention of chemotherapeutic agents (Castro et al., 2003; Duvillard et al., 1999; Wenig et al., 2002) and to use liposomal drug delivery to intratumorally deliver gene therapy (Mattijssen et al., 1994; Nemunaitis et al., 2001; Villaret et al., 2002; Wollenberg et al., 1999; Yoo et al., 2001). In animal studies, epinephrine has been shown to increase intratumoral concentration of cisplatin up to 12 times (Duvillard et al., 1999). In a phase III study of intratumoral cisplatin/epinephrine injectable gel in advanced head and neck cancer, an objective response rate of 34% (21 of 62 patients) was reported, and the side effects were limited to mostly local pain and cutaneous reactions (Castro et al., 2003). Phase I and phase II trials using liposome E1A gene therapy to inhibit the HER-2/neu expression in HNSCC has shown zero dose-limiting toxicities and objective response in clinical studies (Villaret et al., 2002; Yoo et al., 2001).

In this distribution study, we confirm the ability of liposomes to maintain high locoregional retention (mean locoregional retention rate of 65.1 ± 6.8% at 44 h for all rats by planar imaging) in a HNSCC xenograft positive surgical margin model via intraoperative injection. In the actual clinical setting, we expect to deliver high concentration of liposomal therapeutic agents into the tumor following intraoperatively resection, which should provide sustained perioperative treatment. One interesting difference between intraoperative injection of liposomal therapeutic agents versus intratumoral injection without surgery is the absence of the immediate clearance following injection (Bao et al., 2006a; Ning et al., 1999; Rowlinson-Busza et al., 1991). This improved immediate retention can be explained by the inflammation triggered by the surgical resection of the tumor which is known to improve liposome retention and disrupt vascular system by altering the normal intravascular circulation of the liposomes (Jain, 2001). The high locoregional retention rate derived from planar imaging has the advantage of allowing us to acquire information about the ^{99m}Tc-liposome distribution chronologically without euthanizing the rat.

The gamma counter provides the luxury of acquiring accurate quantitative information about individual tissues post-mortem. When the individual tissues (tumor, skin superior to the tumor, muscle inferior, and intracavitary fluid) were counted, the tumor %IA was higher in the cationic liposome groups compared to the neutral liposome groups of the same size. For different liposome groups of the same charge, the intratumoral retention rate was positively correlated with liposome size. When we compared the tumor percent per gram of tissue across the six groups, the 100 nm ^{99m}Tc-cationic liposome group had the highest value. The higher percent per organ and percent per gram of tissue values demonstrated by the ^{99m}Tc-cationic liposomes indicate that they may achieve superior therapeutic efficacy in clinical setting. The improved retention effect of the cationic liposomes may be due to the over-expression of negatively charged groups in the cell membrane of tumor cells thus facilitating their endocytosis (Utsugi et al., 1991; Yang et al., 2004). Moreover, the size of the liposome may influence intratumoral retention on two levels. The larger liposomes are expected to have slower intravascular clearance due to their size; however, we postulate that the smaller liposomes may accelerate intracellular uptake due to more surface to surface contact with the cell membrane.

One weakness with intratumoral injection is that tumor volume and injection technique may influence retention and distribution of liposomes in the tumor tissue. Therefore, the 100 nm ^{99m}Tc-neutral liposome and 100 nm ^{99m}Tc-cationic liposome intracavitary injection groups were studied to demonstrate the passive targeting property of the cationic liposomes without the influence of tumor size or injection technique. The gamma counter data verified that the 100 nm ^{99m}Tc-cationic liposome group had significantly higher ($p < 0.05$) percent per organ and percent per gram of tissue values than the neutrally charged counterpart. The MicroSPECT/CT fusion images (Fig. 5) reinforce the results from gamma counter and illustrate that the ^{99m}Tc-cationic liposome rat had higher intratumoral activity. Furthermore, ^{99m}Tc-cationic liposome rat displayed a more uniform distribution pattern of activity around the tumor. The cold area for the 100 nm ^{99m}Tc-cationic liposome group lies in the inferior aspects of the tumor where the tumor is attached to the musculature. The ^{99m}Tc-neutral liposome rat had only two small hot spots of activity on the superior, left lateral aspect of the tumor, and the remaining activity was distributed around the dorsum and forelimbs area. The ^{99m}Tc-cationic liposome's passive targeting property provides significant therapeutic advantages in treating HNSCC with positive surgical margin. If the tumor is visible and can be injected, the physician could be fairly confident that the cationic liposomes would deliver excellent retention for prolonged treatment. If the margin cannot be reached via injection, cationic liposome could be injected into the surrounding cavity to allow passive targeting property to take effect. The cationic liposomes' superior intratumoral retention ability may benefit the primary tumor; however, in advanced HNSCC, patients often have microscopic disease surrounding the primary tumor (Nag et al., 2005).

The above concern with microscopic disease could be addressed by injection of liposomal therapeutic agents in the intracavitary fluid. For this purpose, the neutral liposomes may be particularly helpful in achieving higher activity in the fluid covering the surgical cavity. This study showed that the 100 nm and 1 μm ^{99m}Tc-neutral liposomes had significantly higher ($p < 0.05$) %IA in the fluid compared to the 100 nm and 1 μm ^{99m}Tc-neutral liposomes respectively. A logical step in handling a case of advanced, unresectable HNSCC would be to inject cationic liposomal therapeutic agents into the tumor to treat the positive margin and inject neutral liposomal therapeutic agents into the surgical cavity to treat microscopic disease. In areas such as the oral cavity and deep neck, perioperative locoregional treatment using fluid filled with liposomal therapeutic agents would require adequate containment of the fluid to prevent tracking outside the treatment area. However, adequate containment could be achieved by trapping the fluid with graft tissues and further limit the patient's movement postoperatively.

Since systemic distribution of activity in major organs was low, the side effects are projected to be very low. The average %IA from planar ROI image analysis in kidney (Fig. 6A) at baseline, 4 h, 20 h and 44 h for all six groups were $0.9 \pm 0.6\%$, $1.8 \pm 0.8\%$, $2.2 \pm 0.7\%$, and $2.2 \pm 0.8\%$ respectively. The 100 nm ^{99m}Tc-cationic liposome group had the highest %IA at any time point ($3.3 \pm 1.3\%$ by planar imaging and $3.8 \pm 0.5\%$ by gamma counter at 44 h). The liver and gastrointestinal tract had even lower activity compared to the kidneys. Organ distribution data highlights the superiority of local administration in minimizing normal tissue toxicity caused by systemic absorption.

One of other possible toxicities in the various anatomical sites around the tumor would be postoperative wound healing. Other common side effects of conventional radiation therapy of the head and neck include mucositis, neuropathy, and bone pain (Pinheiro et al., 2002). Even with the high intratumoral retention rate achieved through intraoperative injection, we still anticipate minor side effects to occur. With regards to the adverse effect profile on local normal tissues, an intratumoral study using cisplatin/epinephrine gel in advanced head and neck cancer demonstrated that the most frequent local toxicities were local pain around injection site and cutaneous reactions (Castro et al., 2003). Most adverse reaction can be managed using appropriate analgesics and conservative wound healing. Furthermore, the typical side effects related to systemic chemotherapy such as emesis and myelotoxicity were rare and limited. We anticipate similar side effect profile for the radionuclide therapy study.

In conclusion, the results from this intraoperative distribution study using ^{99m}Tc-liposomes in an animal HNSCC positive surgical margin indicate that liposomal drug delivery could potentially achieve high intratumoral retention rate and deliver prolonged therapy perioperatively. The side effect profile is projected to be low with minimal systemic spread of the liposomal therapeutic agents from the tumor site. The application of this intratumoral injection method could extend beyond adjuvant therapy; if it demonstrates high efficacy, we could potentially use it as primary therapy for unresectable, advanced HNSCC.

Acknowledgements

This research was partly supported by NIH/National Cancer Institute Cancer Center SPORE grant, 5 P30 CA054174-16, and San Antonio Area Foundation biomedical research grant. Sean X. Wang was supported by Frederic C. Bartter General Clinical Research Center Scholar research stipend.

References

Bao, A., Goins, B., Klipper, R., Negrete, G., Mahindaratne, M., Phillips, W.T., 2003a. A novel liposome radiolabeling method using ^{99m}Tc-"SNS/S" complexes: in vitro and in vivo evaluation. J. Pharm. Sci. 92, 1893–1904.

Bao, A., Goins, B., Klipper, R., Negrete, G., Phillips, W.T., 2003b. ^{186}Re-liposome labeling using ^{186}Re-SNS/S complexes: in vitro stability, imaging, and biodistribution in rats. J. Nucl. Med. 44, 1992–1999.

Bao, A., Goins, B., Klipper, R., Negrete, G., Phillips, W.T., 2004. Direct ^{99m}Tc labeling of pegylated liposomal doxorubicin (Doxil) for pharmacokinetic and non-invasive imaging studies. J. Pharmacol. Exp. Ther. 308, 419–425.

Bao, A., Phillips, W.T., Goins, B., Zheng, X., Sabour, S., Natarajan, M., Ross Woolley, F.R., Zavaleta, C., Otto, R.A., 2006a. Potential use of drug carried-liposomes for cancer therapy via direct intratumoral injection. Int. J. Pharm. 316, 162–169.

Bao, A., Phillips, W.T., Goins, B., McGuff, H.S., Zheng, X., Woolley, F.R., Natarajan, M., Santoyo, C., Miller, F.R., Otto, R.A., 2006b. Setup and characterization of a human head and neck squamous cell carcinoma xenograft model in nude rats. Otolaryngol. Head Neck Surg. 135, 853–857.

Castro, D.J., Sridhar, K.S., Garewal, H.S., Mills, G.M., Wenig, B.L., Dunphy 2nd., F.R., Costantino, P.D., Leavitt, R.D., Stewart, M.E., Orenberg, E.K., 2003. Intratumoral cisplatin/epinephrine gel in advanced head and neck cancer: a multicenter, randomized, double-blind, phase III study in North America. Head Neck 25, 717–731.

Chen, T.Y., Emrich, L.J., Driscoll, D.L., 1987. The clinical significance of pathological findings in surgically resected margins of the primary tumor in head and neck carcinoma. Int. J. Radiat. Oncol. Biol. Phys. 13, 833–837.

Duvillard, C., Benoit, L., Moretto, P., Beltramo, J.L., Brunet-Lecomte, P., Correia, M., Sergent, C., Chauffert, B., 1999. Epinephrine enhances penetration and anti-cancer activity of local cisplatin on rat sub-cutaneous and peritoneal tumors. Int. J. Cancer 81, 779–784.

Freeman, S.B., Hamaker, R.C., Singer, M.I., Pugh, N., Garrett, P., Ross, D., 1990. Intraoperative radiotherapy of head and neck cancer. Arch. Otolaryngol. Head Neck Surg. 116, 165–168.

Gabizon, A., Catane, R., Uziely, B., Kaufman, B., Safra, T., Cohen, R., Martin, F., Huang, A., Barenholz, Y., 1994. Prolonged circulation time and enhanced accumulation in malignant exudates of doxorubicin encapsulated in polethylene-glycol coated liposomes. Cancer Res. 54, 987–992.

Grimard, L., Esche, B., Lamothe, A., Cygler, J., Spaans, J., 2006. Interstitial low-dose-rate brachytherapy in the treatment of recurrent head and neck malignancies. Head Neck 28, 888–895.

Haque, R., Contreras, R., McNicoll, M.P., Eckberg, E.C., Petitti, D.B., 2006. Surgical margins and survival after head and neck cancer surgery. BMC Ear Nose Throat Disord. 6, 2.

Harrington, K.J., Rowlinson-Busza, G., Syrigos, K.N., Uster, P.S., Vile, R.G., Stewart, J.S.W., 2000. Pegylated liposomes have potential as vehicles for intratumoral and subcutaneous drug delivery. Clin. Cancer Res. 6, 2528–2537.

Huang, S.K., Lee, K.-D., Hong, K., Friend, D.S., Papahadjopoulos, D., 1992a. Microscopic localization of sterically stabilized liposomes in colon carcinoma-bearing mice. Cancer Res. 52, 5135–5143.

Huang, S.K., Mayhew, E., Gilani, S., Lasic, D.D., Martin, F.J., Papahadjopoulos, D., 1992b. Pharmacokinetics and therapeutics of sterically stabilized liposomes in mice bearing C-26 colon carcinoma. Cancer Res. 52, 6774–6781.

Huang, S.K., Martin, F.J., Jay, G., Vogel, J., Papahadjopoulos, D., Friend, D.S., 1993. Extravasation and transcytosis of liposomes in Kaposi's sarcoma-like dermal lesions of transgenic mice bearing the HIV tat gene. Am. J. Pathol. 143, 1–14.

Jain, R.K., 2001. Delivery of molecular and cellular medicine to solid tumors. Adv. Drug Deliv. Rev. 46, 149–168.

Jesse, R.H., Sugarbaker, E.V., 1976. Squamous cell carcinoma of the oropharynx: Why we fail? Am. J. Surg. 132, 435–438.

Jones, A.S., Bin Hanafi, Z., Nadapalan, V., Roland, N.J., Kinsella, A., Helliwell, T.R., 1996. Do positive resection margins after ablative surgery for head and neck cancer adversely affect prognosis? A study of 352 patients with recurrent carcinoma following radiotherapy treated by salvage surgery. Br. J. Cancer 74, 128–132.

Klibanov, A.L., Maruyama, K., Torchilin, V.P., Huang, L., 1990. Amphipathic polyethyleneglycols effectively prolong the circulation times of liposomes. FEBS Lett. 68, 235–237.

Maeda, H., 2001. SMANCS and polymer-conjugated macromolecular drugs: advantages in cancer chemotherapy. Adv. Drug Deliv. Rev. 46, 169–185.

Maeda, H., Sawa, T., Konno, T., 2001. Mechanism of tumor-targeted delivery of macromolecular drugs, including the EPR effect in solid tumor and clinical overview of the prototype polymeric drug SMANCS. J. Control. Release 74, 47–61.

Mattijssen, V., De Mulder, P.H., De Graeff, A., Hupperets, P.S., Joosten, F., Ruiter, D.J., Bier, H., Palmer, P.A., Van den Broek, P., 1994. Intratumoral PEG-interleukin-2 therapy in patients with locoregionally recurrent head and neck squamous-cell carcinoma. Ann. Oncol. 5, 957–960.

Nag, S., Schuller, D.E., Martinez-Monge, R., Rodriguez-Villalba, S., Grecula, J., Bauer, C., 1998. Intraoperative electron beam radiotherapy for previously irradiated advanced head and neck malignancies. Int. J. Radiat. Oncol. Biol. Phys. 42, 1085–1089.

Nag, S., Koc, M., Schuller, D.E., Tippin, D., Grecula, J.C., 2005. Intraoperative single fraction high-dose-rate brachytherapy for head and neck cancers. Brachytherapy 4, 217–223.

Nemunaitis, J., Khuri, F., Ganly, I., Arseneau, J., Posner, M., Vokes, E., Kuhn, J., McCarty, T., Landers, S., Blackburn, A., Romel, L., Randlev, B., Kaye, S., Kirn, D., 2001. Phase II trial of intratumoral administration of ONYX-015, a replication-selective adenovirus, in patients with refractory head and neck cancer. J. Clin. Oncol. 19, 289–298.

Ning, S., Yu, N., Brown, D.M., Kanekal, S., Knox, S.J., 1999. Radiosensitization by intratumoral administration of cisplatin in a sustained-release drug delivery system. Radiother. Oncol. 50, 215–223.

Pinheiro, A.D., Foote, R.L., McCaffrey, T.V., Kasperbauer, J.L., Bonner, J.A., Olsen, K.D., Cha, S.S., Sargent, D.J., 2002. Intraoperative radiotherapy for head and neck and skull base cancer. Head Neck 25, 217–226.

Rowlinson-Busza, G., Bamias, A., Krausz, T., Epenetos, A.A., 1991. Uptake and distribution of specific and control monoclonal antibodies in subcutaneous xenografts following intratumor injection. Cancer Res. 51, 3251–3256.

Siegal, T., Horowitz, A., Gabizon, A., 1995. Doxorubicin encapsulated in sterically stabilised liposomes for the treatment of a brain tumor model: biodistribution and therapeutic efficacy. J. Neurosurg. 83, 1029–1037.

Stewart, J.C.M., 1980. Colorimetric determination of phospholipids with ammonium ferrothiocyanate. Anal. Biochem. 104, 10–14.

Torchilin, V.P., 2005. Recent advances with liposomes as pharmaceutical carriers. Nat. Rev. Drug Discov. 4, 145–160.

Torchilin, V.P., 2007. Targeted pharmaceutical nanocarriers for cancer therapy and imaging. AAPS J. 9, E128–E147.

Utsugi, T., Schroit, A.J., Connor, J., Bucana, C.D., Fidler, I.J., 1991. Elevated expression of phosphatidylserine in the outer membrane leaflet of human tumor cells and recognition by activated human blood monocytes. Cancer Res. 51, 3062–3066.

Vaage, J., Barbera-Guillem, E., Abra, R., Huang, A., Working, P., 1994. Tissue distribution and therapeutic effect of intravenous free or encapsulated liposomal doxorubicin on human prostate carcinoma xenografts. Cancer 73, 1478–1484.

Villaret, D., Glisson, B., Kenady, D., Hanna, E., Carey, M., Gleich, L., Yoo, G.H., Futran, N., Hung, M.C., Anklesaria, P., Heald, A.E., 2002. A multicenter phase II study of tgDCC-E1A for the intratumoral treatment of patients with recurrent head and neck squamous cell carcinoma. Head Neck 24, 661–669.

Wang, S.X., Bao, A., Herrera, S.J., Phillips, W.T., Goins, B., Santoyo, C., Miller, F.R., Otto, R.A., 2008. Intraoperative ^{186}Re-liposome radionuclide therapy in a head and neck squamous cell carcinoma xenograft positive surgical margin model. Clin. Cancer Res. 14, 3975–3983.

Wenig, B.L., Werner, J.A., Castro, D.J., Sridhar, K.S., Garewal, H.S., Kehrl, W., Pluzanska, A., Arndt, O., Costantino, P.D., Mills, G.M., Dunphy 2nd., F.R., Orenberg, E.K., Leavitt, R.D., 2002. The role of intratumoral therapy with cisplatin/epinephrine injectable gel in the management of advanced squamous cell carcinoma of the head and neck. Arch. Otolaryngol. Head Neck Surg. 128, 880–885.

Winquist, E., Oliver, T., Gilbert, R., 2007. Postoperative chemoradiotherapy for advanced squamous cell carcinoma of the head and neck: a systematic review with meta-analysis. Head Neck 29, 38–46.

Wollenberg, B., Kastenbauer, E., Mundl, H., Schaumberg, J., Mayer, A., Andratschke, M., Lang, S., Pauli, C., Zeidler, R., Ihrler, S., Löhrs, Naujoks, K., Rollston, R., 1999. Gene therapy—phase I trial for primary untreated head and neck squamous cell cancer (HNSCC) UICC stage II-IV with a single intratumoral injection of hIL-2 plasmids formulated in DOTMA/Chol. Hum. Gene Ther. 10, 141–147.

Yang, N., Strom, M.B., Mekonnen, S.M., Svendsen, J.S., Rekdal, O., 2004. The effects of shortening lactoferrin derived peptides against tumour cells, bacteria and normal human cells. J. Peptide Sci. 10, 37–46.

Yoo, G.H., Hung, M.C., Lopez-Berestein, G., LaFollette, S., Ensley, J.F., Carey, M., Batson, E., Reynolds, T.C., Murray, J.L., 2001. Phase I trial of intratumoral liposome E1A gene therapy in patients with recurrent breast and head and neck cancer. Clin. Cancer Res. 7, 1237–1245.